FOCUS REVIEW

WIREs Computational Molecular Science

Exploring High-Dimensional Free-Energy Landscapes of Chemical Reactions

Shalini Awasthi[1]* | **Nisanth N. Nair**[2]†

[1]Department of Chemistry, Indian Institute of Technology, Kanpur, Uttar Pradesh, 208016 , India

Correspondence
Department of Chemistry, Indian Institute of Technology, Kanpur, Uttar Pradesh, 208016 , India
Email: nnair@iitk.ac.in

Present address
*Warwick Manufacturing Group, University of Warwick, Coventry, Warwickshire, CV47AL, United Kingdom

Funding information

Molecular dynamics (MD) techniques are widely used in computing free-energy changes for conformational transitions and chemical reactions, in particular, to study such processes in condensed matter systems. Most of the MD-based approaches employ biased sampling of *a priori* selected coarse grained coordinates or collective variables (CV) and thereby accelerating otherwise infrequent transitions between different free-energy basins. A quick convergence in free-energy estimations can be achieved by enhanced sampling of large number of CVs. Conventional enhanced sampling approaches become exponentially slower with increasing dimensionality of the CV-space, and thus they turn out to be highly inefficient in sampling high-dimensional free-energy landscapes. Here we focus on some of the novel methods that are designed to overcome this limitation. In particular, we discuss four methods: bias exchange metadynamics, parallel bias metadynamics, adiabatic free-energy dynamics/temperature accelerated MD, and temperature accelerated sliced sampling. The basic idea behind these techniques are presented and the applications using these techniques are illustrated. Advantages and disadvantages of these techniques are delineated.

Abbreviations: MD, Molecular Dynamics; AIMD, Ab Initio Molecular Dynamics; CV, Collective Variables; BEMetaD Bias Exchange Metadynamics; PBMetaD, Parallel Bias Metadynamics; AFED, Adiabatic Free Energy Dynamics; TAMD, Temperature Accelerated Molecular Dynamics; TASS, Temperature Accelerated Sliced Sampling

*Equally contributing authors.

KEYWORDS
Free-energy calculations, Enhanced sampling, Bias Exchange Metadyanmics, Parallel-Bias Metadynamics, Adiabatic Free-Energy Dynamics, Temperature Accelerated Sliced Sampling

1 | INTRODUCTION

Free-energy changes along the reaction coordinate of a chemical reaction manifests the feasibility of the process at a given temperature. Reaction coordinate, χ, on the other hand, can be an intricate function of nuclear coordinates even for a simple elementary reaction. To simplify, χ can be written as a linear combination of several coarse grained coordinates or collective variables (CV), $\mathbf{S}$, as,

$$\chi(\mathbf{R}) = \sum_i c_i \, S_i(\mathbf{R}) \ ,$$

where $\mathbf{R}$ is the set of all atomic coordinates, and $\{c_i\}$ is the set of coefficients. Computing the free-energy landscape $F(\mathbf{S})$ and finding the lowest free-energy path $\chi(\mathbf{S})$ on this landscape could provide valuable information regarding the mechanism and kinetics of the reaction.[1, 2] Free-energy calculations using molecular dynamics (MD) simulations are widely used for this purpose, and is the most preferred approach while dealing with soft matter systems. MD based sampling enables one to account for entropic contributions, going beyond the standard quantum-harmonic approximations.

In order to compute $F(\mathbf{S})$, it is important that all the relevant conformational states for a given $\mathbf{S}$ is sampled in MD simulations.[1, 2, 3, 4, 5, 6] On the other hand, probability ($P(\mathbf{R})$) to visit a conformational state $\mathbf{R}$ at temperature T, is proportional to $e^{-\beta U(\mathbf{R})}$, where $U(\mathbf{R})$ is the potential energy, $\beta = 1/(k_B T)$ and k_B is the Boltzmann constant. As a result, high potential regions are less visited or never visited compared to low–potential energy parts of the potential energy landscape in a finite length MD trajectory. Thus barrier crossing on a potential energy landscape turns out to be an infrequent or "rare" event in MD simulations. Even moderately (i.e. only a few $k_B T$) high potential energy regions can be insufficiently sampled, resulting in poor statistics.

This problem can be alleviated by modifying the potential energy surface by adding a bias potential.[2] If the potential energy of the low–potential regions is raised, the barrier crossing events are accelerated. In such biased-sampling simulations, the probability of visiting $\mathbf{R}$ gets modified as,

$$\tilde{P}(\mathbf{R}) \propto e^{-\beta\left[U(\mathbf{R})+V^b(\mathbf{S})\right]} \ .$$

Here $V^b(\mathbf{S})$ is the bias potential added along a selected set of CVs or all the nuclear coordinates. Alternative way to speed-up the exploration of potential energy landscape is by increasing temperature T (i.e., by decreasing β).

For the case of time-independent bias potential $V^b(\mathbf{s})$, the biased probability distribution of CVs, $\tilde{P}(\mathbf{s})$, is related to $P(\mathbf{s})$ as,[7]

$$P(\mathbf{s}) = \tilde{P}(\mathbf{s}) \, e^{\beta V^b(\mathbf{s})} \ ,$$

where

$$\tilde{P}(\mathbf{s}) \equiv \left\langle \prod_i \delta\left(S_i(\mathbf{R}) - s_i\right) \right\rangle_{V^{\mathrm{b}}} ,$$

and $\langle \cdots \rangle_{V^{\mathrm{b}}}$ denotes the ensemble average from the biased MD simulation. Now, from $P(\mathbf{s})$, free-energy surface can be computed as,

$$F(\mathbf{s}) = -\beta^{-1} \ln P(\mathbf{s}) \ . \tag{1}$$

Free-energy surface can be also computed based on integrating the mean-force as

$$\Delta F(s) = \int^{s} ds' \left\langle \left(\frac{dF}{ds'} \right) \right\rangle \ .$$

Biased sampling techniques use different ways to obtain $V^{\mathrm{b}}(\mathbf{s})$ that compensates the underlying free-energy landscape. For e.g. metadynamics[8, 9] constructs the bias potential as a function of time by a time-dependent update of the bias, while umbrella sampling[7] (US) uses time-independent biases to compute $P(\mathbf{s})$ directly. The bias potential is self-consistently obtained in recently developed variational enhanced sampling method.[10] Blue-moon ensemble[11] and Adaptive Bias Force methods (see Ref.[12] and references therein) are two examples which use the biased/unbiased mean-forces to compute free-energy.[2] In adiabatic free-energy dynamics (AFED) [13] $P(\mathbf{s})$ is calculated directly from the high-temperature dynamics of CVs.

Alternatively, equilibrium probability distribution and free-energies can be computed using replica–exchange based global-tempering approaches.[2, 14, 15, 16, 17, 18] In the widely used parallel-tempering approach,[19] exploration of the potential energy landscape is enhanced in a high–temperature replica, while a low–temperature replica exchanges its coordinates with a higher–temperature replica with certain probability. The advantage of global tempering simulations is that *a priori* assumption of CVs is not necessary. Readers are directed to authoritative books[2, 1, 20] and reviews on various sampling methods for further details.[21, 6, 5, 22, 3, 23]

Other than the requirement of *a priori* selection of CVs, the major limitation of the CV-based approaches is its exponentially decreasing computational efficiency with increase in the dimensionality of the CV space. When modeling an elementary reaction, free-energy surface for the process can be often expressed with one or two collective coordinates in a way that free-energy of all the reactant states, transition state and product states can be obtained.[2] However, enhanced sampling of one or two CVs may not be sufficient to compute free-energies accurately, especially for processes in soft-matter systems. This arises from the fact that transverse degrees of freedoms are unbiased and their sampling is slow due to finite barriers prevailing in the orthogonal directions. Therefore, including more orthogonal CVs is beneficial for obtaining reliable free-energy estimates from short MD simulations. Requirement of methods that could enhance the sampling of perpendicular coordinates without loosing the efficiency of the simulation is now comprehensible. This review focuses on four such methods, which are designed to sample large number of CVs efficiently and have been already demonstrated for modeling rare-events in soft matter systems with more than 3 CVs.

2 | BIAS EXCHANGE METADYNAMICS

Metadynamics approach uses a time dependent bias potential to enhance the sampling of the configurational space.[24, 9] Readers can refer to a number of reviews on the topic.[25, 26, 27, 28, 29, 22, 30, 21] The bias potential has the form

$$V^{\mathrm{b}}(\mathbf{S}, t) = \sum_{\tau<t} w(\tau) \exp\left[-\frac{(\mathbf{S}-\mathbf{S}_\tau)^2}{2\,(\delta s)^2}\right]$$

which is the sum of Gaussian functions deposited along the trajectory of $\mathbf{S}$ at discrete time τ. Here, w is the height of the Gaussian (in the units of energy) and δs is the width parameter. The Lagrangian for performing metadynamics is

$$\mathcal{L}^{\mathrm{MTD}}(\mathbf{R}, \dot{\mathbf{R}}) = \mathcal{L}_0(\mathbf{R}, \dot{\mathbf{R}}) - V^{\mathrm{b}}(\mathbf{S}, t) \ ,$$

where $\mathcal{L}_0$ is the unbiased Lagrangian of the system. The bias potential V^{b} that compensates the underlying potential is gradually built along the trajectory of CVs. As the bias flattens the free-energy basin, the system exits from one free-energy basin to the other. Most importantly, in metadynamics, the free-energy surface can be computed from the bias potential itself, as

$$F(\mathbf{S}) = -V^{\mathrm{b}}(\mathbf{S}, t \to \infty) + \text{ constant} \ .$$

In a simple metadynamics procedure the Gaussian parameters w_τ and δs are fixed. However, there are procedures to change these parameters adaptively for obtaining proper convergence in free-energy estimates. [31, 32] Most importantly, the well–tempered version of metadynamics scales $w(\tau)$ based on the underlying bias potential V^{b} at time τ:[31]

$$w(\tau) = w(0) \exp\left(-\frac{V^{\mathrm{b}}(\mathbf{S}, \tau)}{k_{\mathrm{B}} \Delta T}\right) \ ,$$

where $w(0)$ is initial Gaussian height and ΔT is the tempering parameter. In well-tempered metadynamics, free-energy can be computed as[31, 33]

$$F(\mathbf{S}) = -\gamma V^{\mathrm{b}}(\mathbf{S}, t \to \infty) + \text{ constant},$$

where $\gamma = (T + \Delta T)/\Delta T$.

In principle, the method requires no modification to sample large number of CVs. However, the number of Gaussian functions require to build the bias that compensates the underlying free-energy surface increases exponentially with the system size. In practice, metadynamics is used to sample low dimensional landscapes, most often using 2 CVs, rarely with 3 CVs, and in some special cases even higher;[27] see also Ref. [34].

In order to improve the efficiency of metadynamics in sampling high-dimensional free-energy surfaces, bias-exchange metadynamics (BEMetaD) approach was proposed by Piana and Laio.[35] In this approach, M number of replicas of the system at same temperature are initiated, and in each of these replicas, different small number of CVs are enhance-sampled using metadynamics bias built independently in each replica. Exchanges between randomly chosen two replicas are then attempted at regular time intervals, as in the case of other replica exchange MD schemes; see Figure 1. Each replica samples one or two dimensional CV space, therefore sampling a high-dimensional space becomes

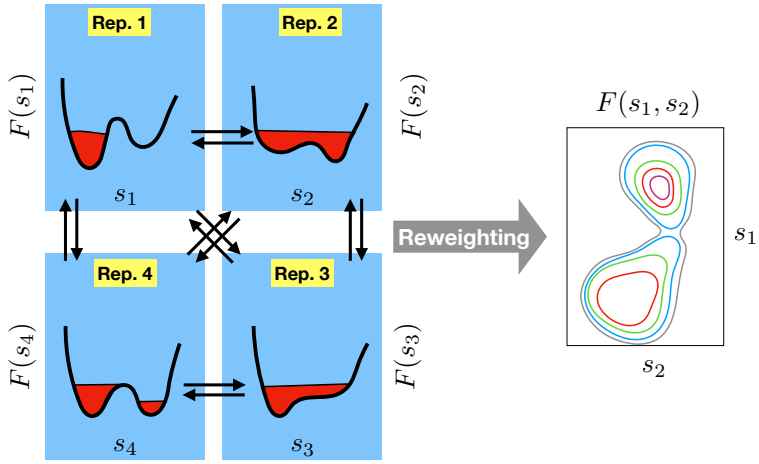

FIGURE 1 A sketch demonstrating the basic idea behind the BEMetaD method. Here the arrows are showing exchanges between two randomly selected replicas, which are attempted frequently. The bias added is shown in red. A reweighting procedure could be used to reconstruct a high-dimensional free-energy surfaces.

highly efficient. By the virtue of this, the efficiency of sampling doesn't deteriorate exponentially with the number of CVs.

Exchange between two replicas m and n are made with the probability $P_{m,n}$ using the Metropolis-Hastings scheme, where

$$P_{m,n} = \min\left(1, \exp\left[\beta \Delta_{m,n}\right]\right)$$

and

$$\begin{aligned} \Delta_{m,n} &= V_m^{\mathrm{b}}\left[S_m(\mathbf{R}_m), t\right] - V_m^{\mathrm{b}}\left[S_m(\mathbf{R}_n), t\right] \\ &+ V_n^{\mathrm{b}}\left[S_n(\mathbf{R}_n), t)\right] - V_n^{\mathrm{b}}\left[S_n(\mathbf{R}_m), t\right] \quad . \end{aligned}$$

A later work by Galvelis and Sugita[36] has shown that exchange rates between two replicas and the convergence of free-energies can be expedited by using infinite swapping or the Suwa-Todo (ST) algorithms, replacing the Metropolis-Hastings scheme.

Reconstructing the high-dimensional free-energy surface requires appropriate reweighting; see Refs. [35, 37] for details. The unbiased probability contribution due to the bias from a replica h can be written as

$$P_h(\mathbf{s}) = \left\langle \prod_i \delta(S_i - s_i)\, e^{\beta\left[\overline{V}_h^b(S_h) - f_h\right]} \right\rangle \quad .$$

Here, $\overline{V}^b_h(S_h)$ is the average bias potential in replica h, given by

$$\overline{V}^b_h(S_h) = \frac{1}{t_{\text{final}} - t_{\text{ini}}} \int_{t_{\text{ini}}}^{t_{\text{final}}} dt\, V^{\text{b}}_m(S_h, t)$$

where the reweighting is done for a time interval t_{ini} and t_{max} during which the average bias potential only increases uniformly across the domain of **S** of our interest. In the above, f_h is some constant, and has to be determined. Now, using the weighted histogram analysis method[38] (WHAM) one can combine $\{P_h(\mathbf{s})\}$ to get the total reweighted probability density $P(\mathbf{s})$, and hence the free-energy $F(\mathbf{s})$. A detailed review of the method and other technical details can be found in Ref. [37]. Laio and co-workers have also designed a visual interface program for reweighting and analysis of PBMetaD simulations.[39] Another simpler approach for reweighting was suggested by Yu and Lin [40], where a standard time-independent reweighting is done using the converged free-energies $F_h(S_h)$.

Alternatively, time dependent bias can be directly used for reweighting following the works of Tiwary and Parrinello. [6] Here,

$$P_h(\mathbf{s}) = \left\langle \prod_i \delta(S_i - s_i)\, e^{\beta\left[V^b_h(S_h,t) - c_h(t)\right]} \right\rangle \quad . \tag{2}$$

where $c_h(t)$ is a time dependent constant, given by

$$c_h(t) = \beta^{-1} \ln \left[\frac{\int dS_h\, e^{\beta\gamma V^{\text{b}}_h(S_h,t)}}{\int dS_h\, e^{\beta(\gamma-1)V^{\text{b}}_h(S_h,t)}} \right]$$

considering that a well-tempered bias potential is used. Employing WHAM, one can then combine the reweighted free-energy surfaces from each replica h, similar to the procedure used by Awasthi et al. [41]. It is noted that the WHAM approach for combining the distributions of different replicas can only work if the distributions have enough overlap.

A number of applications using BEMetaD in studying biological systems can be found in the literature. Piana and Laio [35] employed 5 CVs to study the folding of Trp-Cage in explicit water. They used number of C_γ contacts (CV1), number of C_α contacts (CV2), number of backbone H-bonds (CV3), number of backbone ψ dihedrals within the α-domain of the Ramachandran map (CV4), and correlation between the successive ψ-dihedral angles (CV5). These simulations were performed with 8 replicas, where 5 replicas were using one-dimensional biases to sample one of the five CVs. Two replicas were using a two-dimensional bias to sample (CV3,CV4) and (CV4,CV5) CV-space. The last replica was a neutral one, i.e. without any bias, and it was permitted to exchange with other walkers. The neutral replica was used to monitor the convergence, which in principle should result in a canonical distribution. In their work, within 20 ns, convergence in free-energy was observed. Free-energy profile along different CVs are given in Figure 2. The trajectories from these simulations have been used to perform cluster analysis and the folding kinetics has been obtained.[42]

A number of different problems have been studied by BEMetaD. For sampling various conformations of chromophores attached to a protein, Delor et al.[43] used BEMetaD. Structural changes in RNA nucleotides and ligand binding were studied using this approach by Mlýnský and Bussi.[44] BEMetaD was used for investigating more complex problems like DNA G-Quadraplex [45] folding, and formation of RNA pseudoknot[46]. Ligand and drug association and dissociation studies in proteins [47, 48, 48, 49, 50, 51, 52, 53, 54], peptides [55] and lipids[56] and conformations of protein:ligand complex[57] have been also carried out using this method. BEMetaD simulation of ion binding in RNA [58] has been recently reported. A number of studies used BEMetaD to study protein folding. [59, 60, 61, 62, 63, 64, 65, 66, 67] Literature of BEMetaD also includes conformational sampling in α-helical

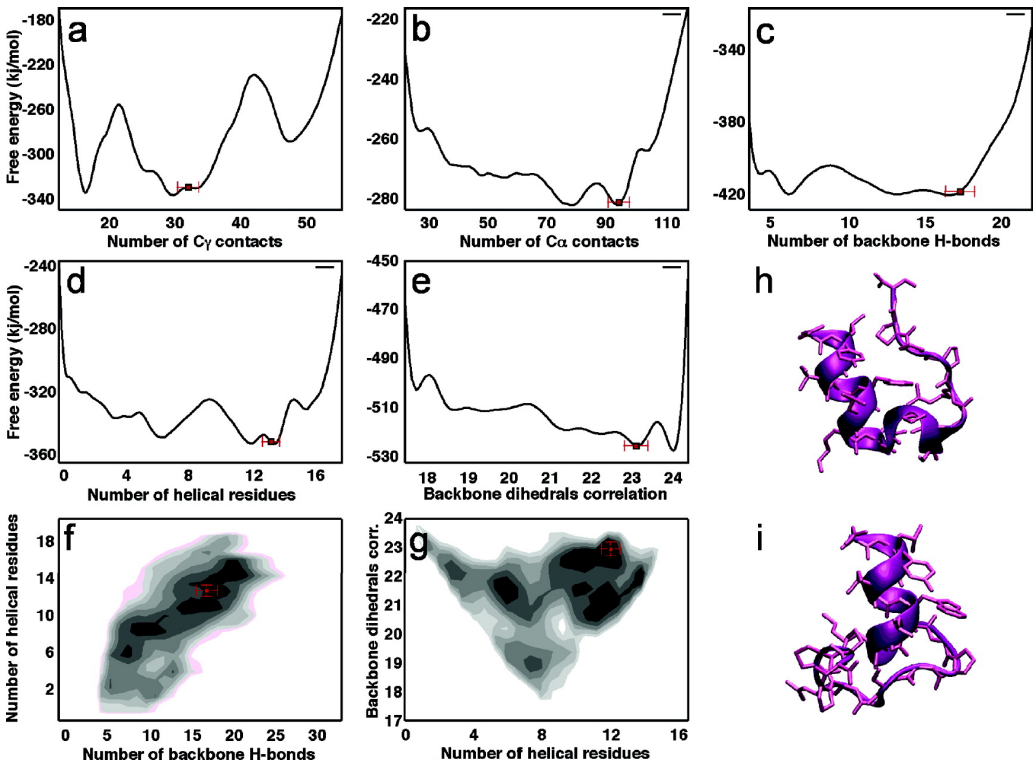

FIGURE 2 (a-g) Free-energy profiles along different CVs used in the BEMetaD simulation of Trp-cage protein folding.[35] These free-energy profiles are made based on the metadynamics bias constructed in each replica; Figures (h,i) are the structures of the folded and the "pseudo-folded" states of the protein. Reprinted with permission from J. Phys. Chem. B 2007;111:4553 Copyright (2018) American Chemical Society

glycoproteins [68], Bovine Chymosin [69], peptides [70, 40, 71], conformational sampling of intrinsically disordered as well as other proteins [72, 73, 74, 75, 76, 77, 78, 79, 80, 81, 82, 83, 84, 85, 86, 87, 88, 89, 90], conduction through ion channels [91, 92, 93, 94, 95], and protein aggregation. [96, 97, 98] The method has also helped to resolve the structure of large and complex systems like protein-RNA complex [99], and membrane inserted influenza fusion peptide [100]. Clearly, a substantial number of complex biophysical problems have been addressed by the approach.

One of the major limitations of this approach is the requirement of the replica-exchange. Care should be given to achieve a proper overlap of probability distributions between the replicas. These limit BEMetaD computations to be used for studying chemical reactions in *ab initio* molecular dynamics (AIMD) where computationally expensive first-principle based QM forces are used to propagate the atomic motion. Study of chemical reactions using BEMetaD and AIMD has not been reported so far.

3 | PARALLEL BIAS METADYNAMICS

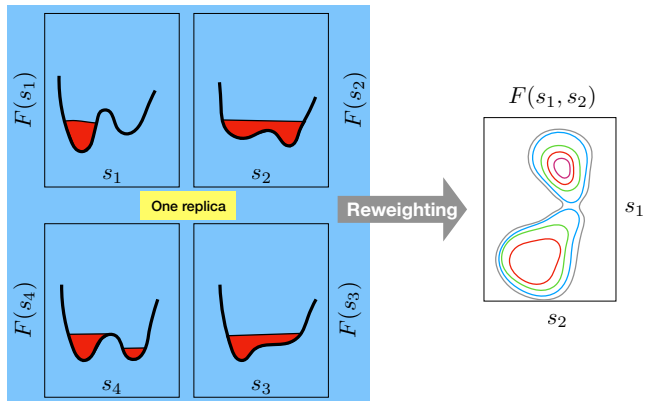

FIGURE 3 Sketch showing the working of PBMetaD. Here, low-dimensional free-energy surfaces are sampled parallelly within the same replica. Gaussian height of the bias added along one CV is scaled according to the bias added along other CVs. Reweighting methods can recover the high-dimensional free-energy landscapes.

Another variant of metadynamics method called the Parallel Bias metadynamics (PBMetaD)[101] alleviates some of the limitations of BEMetaD. In this method low-dimensional (usually one-dimensional) biases are added along CVs concurrently. Only one replica of the system is considered. To ensure that the one-dimensional bias potentials added on different one-dimensional CVs converge to the correct free-energy, bias potential along each CV is dynamically scaled. The Gaussian height at a time τ for a CV i is computed as

$$w_i(\tau) = w_i(0) \exp\left(-\frac{V_i^{\mathrm{b}}(s_i, \tau)}{k_{\mathrm{B}}(\Delta T)_i}\right) p_i(\tau)$$

with

$$p_i(\tau) = \frac{\exp\left(-\beta V_i^{\mathrm{b}}(s_i,\tau)\right)}{\sum_i \exp\left(-\beta V_i^{\mathrm{b}}(s_i,\tau)\right)}$$

Here $V_i^{\mathrm{b}}(s_i,\tau)$ is the total bias for a CV i at a time t. These biases are constructed in the same way as in the conventional well-tempered metadynamics. The effective bias acting on the system at a time t is

$$V_{\mathrm{PB}}^{\mathrm{bias}}(\mathbf{s},t) = -\beta^{-1}\ln\left[\sum_i \exp\left(-\beta V_i^{\mathrm{b}}(s_i,t)\right)\right] + V_0$$

where $V_0 = \beta^{-1}\ln 2$ is added to avoid negative bias. Free-energy along a CV s_i can be computed as

$$F(s_i) = -\gamma \lim_{t\to\infty} V_i^{\mathrm{b}}(s_i,t) \ .$$

High-dimensional free energy surfaces can be also reconstructed by reweighting the trajectory from a fixed-bias simulation or employing the the Tiwary-Parrinello[6] reweighting (with appropriate modifications) using the dynamic bias $V_{\mathrm{PB}}^{\mathrm{b}}(\mathbf{s},t)$.

The major advantage compared to BEMetaD is that only one-replica is used for biasing more than one CVs. Especially, replica exchange is avoided in the approach.

Pfaendtner and Bonomi have used this approach in studying the conformational changes in the Tryp-cage protein with implicit solvent.[101] Authors have used six CVs with each CV being biased with one-dimensional bias potentials. The CVs chosen were number of C_γ contacts, number of backbone H-bonds, α-helicity, β-similarity, correlation between the successive backbone dihedral angles, and radius-of-gyration. They compared the performance of the method with BEMetaD and it was found that the free-energy convergence behavior of PBMetaD is as good as BEMetaD. BEMetaD together with the Metadynamic Metainterface method was used to explore the structural ensembles of ligand-association in a disordered protein.[102, 103] Conformational sampling of peptoids at the hyrophobic and hydrophilic surface-water interface was modeled by Prakash et al.[104]

Recently, PBMetaD was used to obtain the reaction network of decomposition of γ-ketohydroperoxid.[105] In this work, Fu and Pfaendtner used the SPRINT (social permutation invariant) collective coordinates[106] as CVs for sampling different reaction pathways. SPRINT coordinates allows one to explore the potential energy landscape and the reaction pathways with least chemical knowledge and input. On the other hand, one SPRINT CV per atom is required and thus for a reasonably large system, the number of coordinates become very large and efficient sampling by conventional approaches become difficult. Since PBMetaD enables parallel sampling of one-dimensional CVs with one-dimensional MetaD biases, the method is well suited to sample large number of SPRINT CVs. Authors have used the PM6 method within the AMBER program to sample 12-CVs. The obtained reaction pathways were then refined using static QM calculations; see Figure 4.

4 | ADIABATIC FREE-ENERGY DYNAMICS AND TEMPERATURE ACCELERATED MOLECULAR DYNAMICS

Rosso et al. [13, 107, 2] proposed a very unique enhanced sampling scheme called adiabatic free-energy dynamics (AFED) that relies on temperature accelerated sampling of CVs. In AFED, enhanced sampling of CVs is achieved by

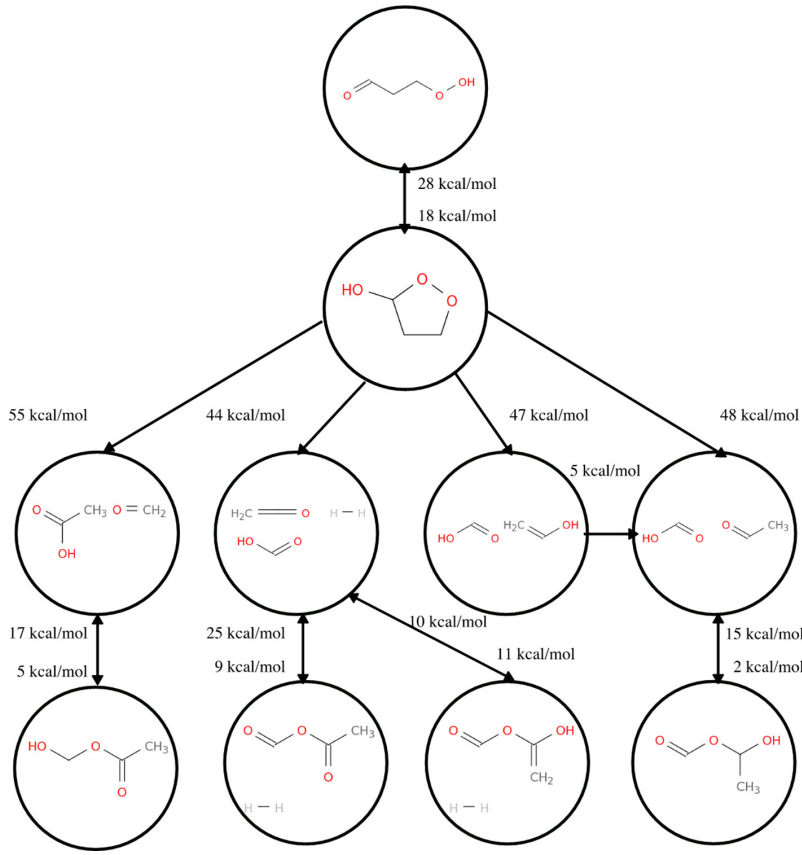

FIGURE 4 Reaction pathways of γ-ketohydroperoxid explored by PBMetaD.[105] Reprinted with permission from J. Chem. Theory Comput. 2018;14:2516 Copyright (2018) American Chemical Society.

introducing high temperature $\tilde{T}$, such that $\tilde{T} \gg T_0$ for n CV degrees of freedom while the remaining degrees of freedom are maintained at the desired physical temperature T_0. In particular, the temperature $\tilde{T}$ is chosen such that CVs can cross the high energy barriers on the potential energy landscape. It is, however crucial that energy flow from the "hot" CV degrees of freedom to the rest of the "cold" nuclear degrees of freedom is avoided. Adiabatic separation between the two subsystems is achieved by choosing a larger mass for the CV degrees of freedom compared to the rest of the nuclear degrees of freedom. Further thermostats are coupled to maintain the temperature of the two subsystems. Under the condition of adiabatic decoupling it was shown that free-energy along the CVs, $F(\mathbf{S})$, at T_0 can be constructed directly from the probability distribution $\tilde{P}(\mathbf{S})$ as, [13, 2]

$$F(S_1, \cdots, S_n) = -\frac{1}{\tilde{\beta}} \ln \tilde{P}(S_1, \cdots, S_n) + \text{ constant } , \tag{3}$$

where $\tilde{\beta} = 1/(k_B \tilde{T})$. The advantage of this approach is that sampling efficiency does not scale exponentially with

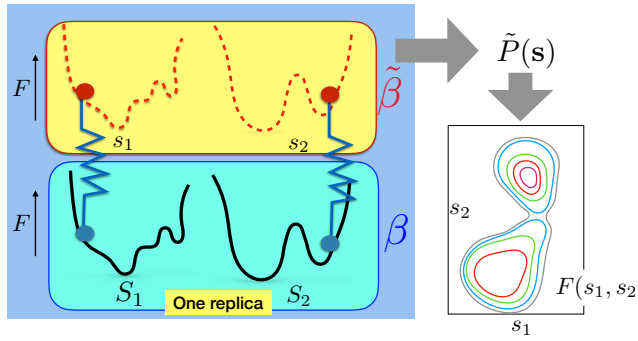

FIGURE 5 Basic idea behind the TAMD/d-AFED method is shown graphically. Here, auxiliary variable **s** are introduced and are coupled with the CVs **S** with a harmonic potential. The **s** degrees of freedom are connected to a thermostat with inverse temperature $\tilde{\beta}$ while the physical system coordinates **S** are thermostatted to an inverse temperature β, with $\tilde{\beta} << \beta$. Free-energy of the system at β along the CVs can be computed directly from the probability distribution of **s** at $\tilde{\beta}$.

the dimension of the CV-space, especially when the changes along the CVs are uncorrelated. However, enhance-sampling of the CV subspace from the full coordinate-space requires coordinate transformation from Cartesian to CV. Implementation of such transformation is not straightforward for many non-linear CVs and the method requires major changes in an existing MD code.

Maragliano et al. [108] alleviated the problem of coordinate transformation in AFED by introducing an extended Lagrangian scheme, like in Ref.[9], and reformulated AFED in the extended CV-space. This method is called Temperature Accelerated MD or driven-AFED (TAMD/d-AFED) [108, 109]. Here a set of auxiliary variables $\{s_\alpha\}$ are introduced that are coupled with the CVs $\{S_\alpha\}$ through a harmonic potential having force constant k_α. The Lagrangian for TAMD/d-AFED is,

$$\mathcal{L}_{\text{TAMD}}(\mathbf{R}, \dot{\mathbf{R}}, \mathbf{s}, \dot{\mathbf{s}}) = L_0(\mathbf{R}, \dot{\mathbf{R}}) + \sum_{\alpha=1}^{n} \frac{1}{2} \mu_\alpha \dot{\mathbf{s}}_\alpha^2 - \sum_{\alpha=1}^{n} \frac{k_\alpha}{2} (S_\alpha - s_\alpha)^2 \ . \tag{4}$$

Here, the auxiliary subsystem $\{s_\alpha\}$ is thermostatted to a high-temperature $\tilde{T}$, while the physical system is thermostatted to a much lower temperature T_0. The mass for the auxiliary variables (μ_α) is taken to be much larger than the atomic masses in the system to ensure adiabatic decoupling of the auxiliary variables from the rest of degrees of freedom. Tuckerman et al. [2, 109, 110] have shown that

$$F(s_1, \cdots, s_n) = -\frac{1}{\tilde{\beta}} \ln \tilde{P}(s_1, \cdots, s_n) \ . \tag{5}$$

Here $\tilde{P}(\mathbf{s})$ is the probability distribution of $\{s_\alpha\}$ of the auxiliary system at temperature $\tilde{T}$.

Number of different applications using TAMD/d-AFED have been reported in the literature. Abrams et al. [112]

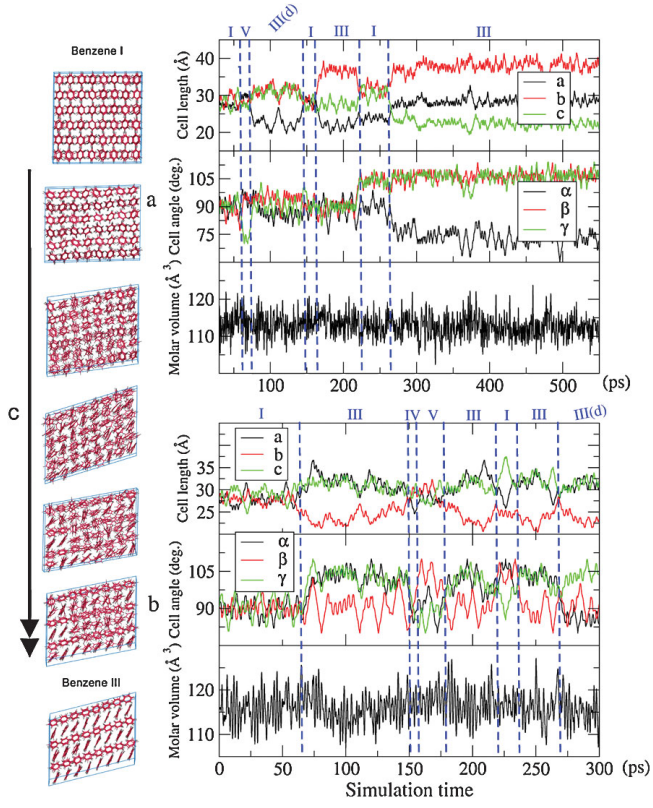

FIGURE 6 Changes in the crystal structures of benzene explored by TAMD/d-AFED.[111] Reprinted figure with permission from Yu, TQ and Tuckerman, ME, Phys. Rev. Lett., 107, 015701, 2011. Copyright (2018) by the American Physical Society.

employed TAMD/d-AFED for studying large–scale conformational sampling of proteins. In this study, they considered 69 CVs to enhance the conformational transitions which involve rotational as well as translation motion of domains in HIV–1 gb120. All the CVs were thermostated at 6 kcal/mol. For studying the conformational changes in the activation–loop of the insulin receptor kinase domain, Vashisth et al. [113] used TAMD/d-AFED. Maragliano et al. [114] and Lapelosa et

al. [115] used this method to study the CO migration in Myoglobin. Tzanov et al. [116] and Cortes-Ciriano et al. [117] used this approach to predict peptide conformations. TAMD/d-AFED and the Monte-Carlo version of TAMD were employed to study vacancy diffusion in crystals, [118] wherein very complex CVs were used such as moments computed by the quantum-mechanical (QM) probability density of a pseudo probe particle. In an another interesting application of TAMD, 720 three-dimensional vectorial CVs were used to sample the conformational changes in hydrated Nafion polymeric system. [119] Yu and Tuckerman have extended the TAMD/d–AFED approach to study crystal structure changes.[111] This was achieved by using supercell vectors or **h**-matrix elements as the CVs in a flexible-cell NPT ensemble MD simulation. This approach was shown to be very efficient in sampling crystal structures, including organic crystals.[120, 121, 122, 123] In Figure 6, TAMD/d-AFED trajectories exploring crystal structures of benzene at 100 K and 2 GPa are shown.[111] In that work,[111] **h** matrix elements were used as the CVs and $\bar{T}$ of 31000 K was taken for enhancing the conformational changes between different polymorphs of benzene. It is worth noting that TAMD/d-AFED combined with DFT based AIMD was used by Samanta et al. [122] to study the melting of high-pressure phase of SiO_2. To improve the efficiency of sampling by TAMD/d–AFED, Tuckerman and co–workers [124] integrated it with biased sampling of CVs, which they named as the Unified Free-Energy Dynamics (UFED) method. In UFED, high temperature and bias potential were simultaneously applied on all the CVs. TAMD/d-AFED and UFED methods have been used to compute accurate mean-forces and then used to optimize structures and reaction pathways on free-energy surfaces.[125, 126] These techniques were also used to compute free-energy differences between two conformations or structures by combining with alchemical free-energy perturbation methods [127, 128] and by calculating free-energies along an arbitrary pathway which connects two conformations.[129]

5 | TEMPERATURE ACCELERATED SLICED SAMPLING

In many chemical reactions, broad and unbound free-energy surfaces can be seen along the crucial "reactive" CVs; see Figure 7. Ideal examples include free-energy profile for A+B type reaction (along A-B distance), drug binding (along drug-active site distance), and protein-folding (along end-to-end distance). As a result, the system will be driven towards uninteresting regions of the free-energy landscape during the enhanced sampling simulations. Thus, the reaction of interest may not be observed or might require long MD simulations. This issue becomes more serious while modeling chemical reactions using AIMD, since the free-energy estimations with AIMD have to be carried out within few tens of picoseconds.

Methods based on metadynamics and TAMD/d-AFED suffer from this problem. A controlled sampling of CVs is crucial to overcome this limitation. This could be achieved by US [7] where the CVs are restrained at different CV positions, and probability along the CV is obtained by combining the biased-probabilities from different umbrella-windows using WHAM [130, 38] or other methods.[131, 2] However, standard US is often performed using one CV. In that case, transverse coordinates may relax slowly leading to slow converge of free-energy estimates, as discussed earlier.

To overcome this problem, Awasthi et al. combined US with metadynamics (which we termed as "well-sliced metadynamics"), where the CV along which a flat unbound free-energy surface is expected is sampled by US in a controlled manner, while the orthogonal coordinates are sampled by well-tempered metadynamics. [41] Well-sliced metadynamics approach was then extended to accommodate large-number of CVs, by combining it with TAMD/d-AFED approach.[132] This method is called Temperature Accelerated Sliced Sampling (TASS). In TASS, the following

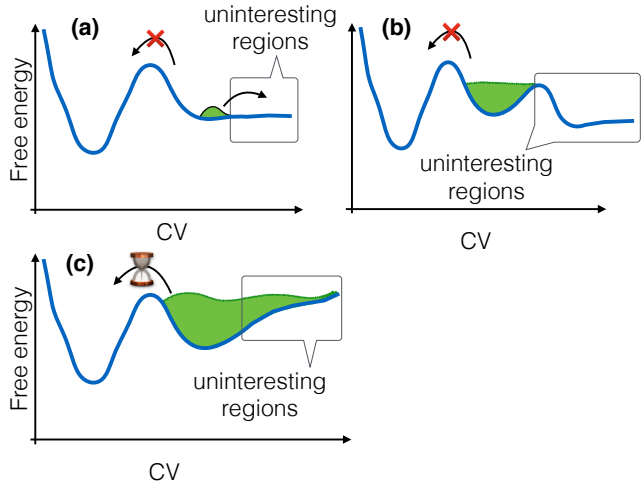

FIGURE 7 A cartoon showing the issues with metadynamics sampling when the free-energy surface along the crucial reactive CV is broad and unbound.[41] Reprinted figure with permission from J. Comput. Chem., 37, 1413, 2016. Copyright (2018) by the John Wiley and Sons.

extended-Lagrangian is used:

$$\begin{aligned}\mathcal{L}_h(\mathbf{R},\dot{\mathbf{R}},\mathbf{s},\dot{\mathbf{s}}) \quad &= \quad \mathcal{L}_{\text{TAMD},h}(\mathbf{R},\dot{\mathbf{R}},\mathbf{s},\dot{\mathbf{s}}) \\ &\quad -W_h^{\text{b}}(s_1) - V_h^{\text{b}}(s_2,t)\end{aligned}$$

where $h = 1, \cdots, M$ number of umbrella-windows are considered. The extended Lagrangian approach used here is similar to the TAMD/d-AFED method discussed in the previous section. All the auxiliary variables are coupled to a high temperature bath and nuclear degrees of freedom are thermostatted to a physically relevant colder temperature. Mass μ_α of an auxiliary variable is taken much higher than the nuclear mass to ensure adiabatic separation between the auxiliary and the nuclear subsystems. The main difference to the TAMD/d-AFED method is that, umbrella-bias $W_h(s_1) = \frac{1}{2}\kappa_h\left(s_1 - s_1^0\right)^2$ is applied along one of the CVs, while one or more other CVs are chosen to sample by the metadynamics bias V^{b}. Thus for each umbrella window h, transverse CVs are enhance-sampled by both metadynamics bias as well as high-temperature. The CVs that are not biased by W_h and V_h^{b} are enhanced only by high temperature (as in TAMD/d-AFED). A cartoon showing the basic working principle behind the TASS method is given in Figure 8.

In this way, TASS samples a high-dimensional slice of the free-energy surface along the US coordinate. Biased probability distribution obtained from each slice h, $\tilde{P}_h(\mathbf{s})$, is then reweighted, as in Eqn (2), and then combined using the WHAM method; see Ref.[132, 41] for more details. As in the TAMD/d-AFED method, free-energy can be obtained using Eqn (5).

Thus, this method can be viewed as an improvement over metadynamics and TAMD/d-AFED as it can sample flat, broad, and unbound surfaces in an efficient manner, and it has the advantage that large number of transverse CVs can be sampled like in TAMD/d-AFED. TASS can also be considered as an improvisation of the US method by enabling sampling of large number of orthogonal CVs in a simultaneous manner, thus achieving quick convergence in free-energy

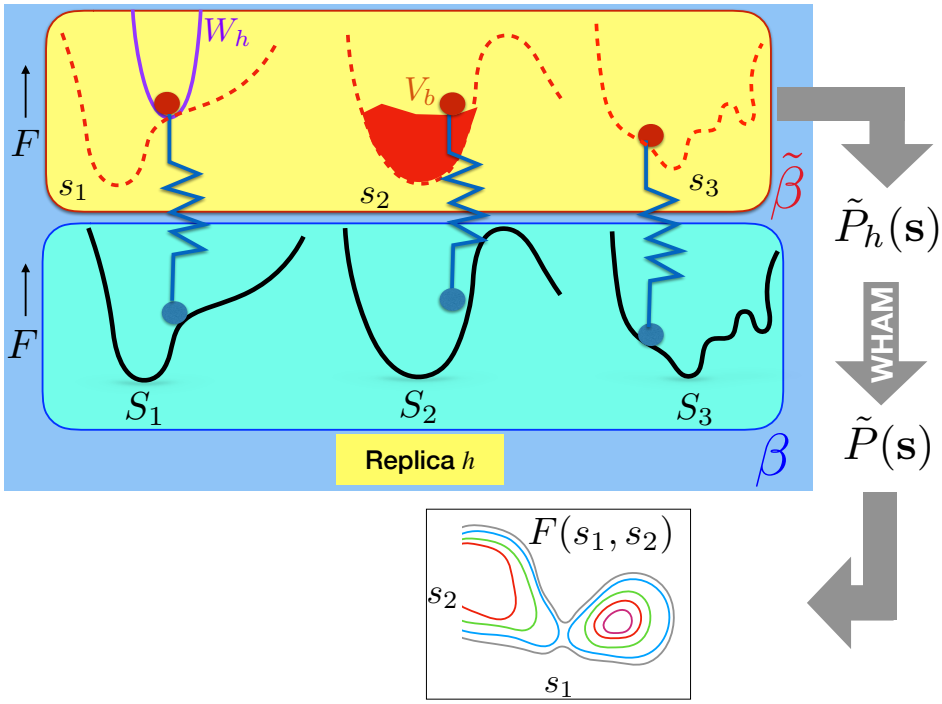

FIGURE 8 A schematic representation on the working principle of the TASS method is shown for a case with three CVs S_1, S_2, and S_3. Note that for $h = 1, \cdots, M$ number of replicas with different umbrella bias $W_h(s_1)$, MD simulations are performed independently. Here metadynamics bias potential (V_b) is applied along s_2 (only). All the auxiliary variables $\{s_\alpha\}$ are connected to a thermostat with inverse temperature $\tilde{\beta}$ and the physical system is thermostatted to an inverse temperature β, with $\tilde{\beta} << \beta$.

estimates. Furthermore, TASS has the flexibility to choose different orthogonal CVs for different umbrella windows. This feature is particularly useful when studying complex chemical reactions where the crucial transverse coordinates change with the progress of the reaction along the "reactive" CV (which is the US CV in most of the cases).

Awasthi and Nair have showed the applicability of the method for computing free energy surfaces of chemical reactions in AIMD and hybrid QM/MM MD simulations.[132] Free-energy surface of alanine tripeptide was also mapped using 4 CVs, and free-energies were showing good convergence within 10 ns per umbrella window (and 31 umbrella windows were used).[132] Awasthi et al. [133] used TASS to study deacylation and reverse acylation reactions of Aztreonam drug catalyzed by class-C β lactamase enzyme. These simulations were using DFT based QM/MM MD methods. For studying the reverse acylation reaction, i.e. **EI** → **ES** in Figure 9, authors used eight CVs. In this reaction C_2 makes a bond with N_1 and recyclize the β-lactam ring; see Figure 9 for labeling. Several conformational changes of the side-chains of the active site ligands are anticipated during this reaction. As these conformational changes are likely to be infrequent events (at least within the small timescale accessible for the QM/MM simulations), enhance sampling of these events were also carried out by appropriate choice of CVs. Two different proton transfer routes were also probed with the CVs considered. The distance $d[\mathrm{AztN_1} - \mathrm{AztC_2}]$ (CV1) was chosen for the US bias, as this CV samples the recylization of the β-lactam ring. At the same time, a broad free energy basin is expected along this CV since different

conformations of the ring-opened drug is possible in the **EI** state. Another CV (CV2), namely the coordination of $AztN_1$ to its hydrogen and to the hydrogen atoms of the active site water W_1 ($C[AztN_1 - \{AztN_1H_1, W_1H\}]$), was chosen for biasing with one-dimensional metadynamics bias. This choice was made as relatively high free-energy barrier is expected for covalent-bond breaking and the free-energy surface along CV2 should have a bound and narrow topology. Temperature of the auxiliary variables was set to 1000 K while the system temperature was kept at 300 K. In total 16 umbrella windows were placed at equal distance from 1.3 to 2.9 Å along CV1. It was observed that the free-energy barrier converges within 9 ps (per umbrella window).[133] The converged free energy surface was computed using the reweighting procedure explained in Ref. [132] and then projected to CV1 and CV2 as shown in Figure 9.

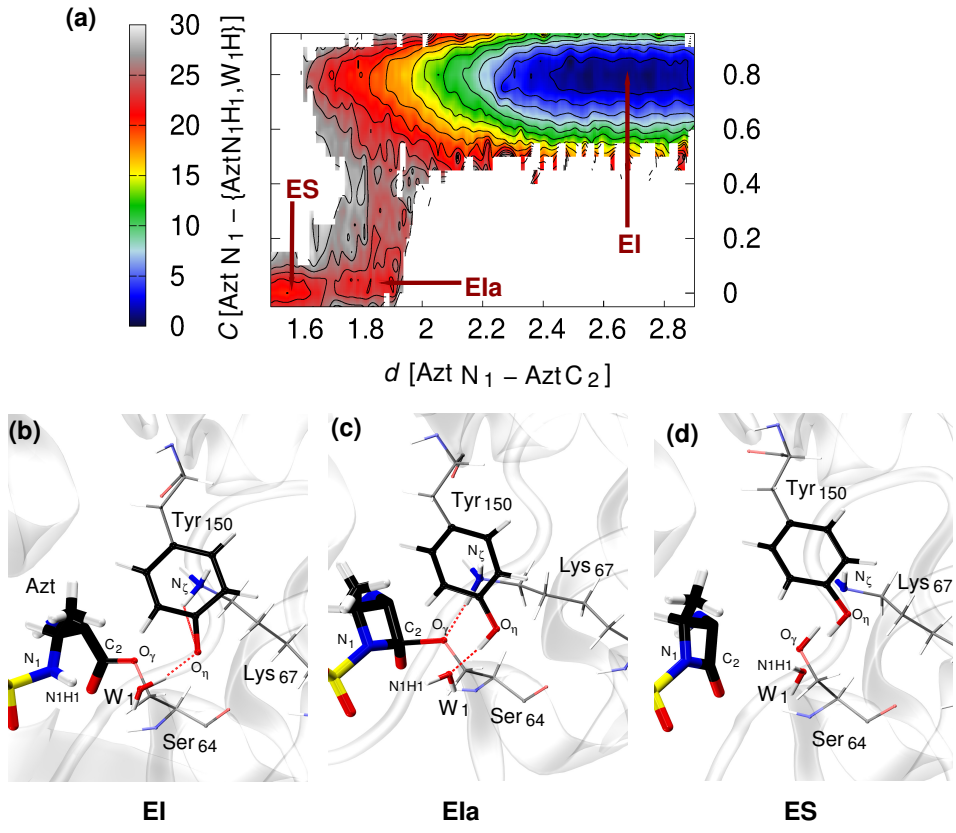

FIGURE 9 Free-energy surface for the reverse acylation of the aztreonam drug catalyzed by class-C β lactamase enzyme is shown. Here the nine-dimensional free-energy surface is projected to CV1-CV2 space. Contour lines are drawn at 2 kcal mol^{-1} intervals. Sub-figures (b), (c), and (d) show representative snapshots of **EI**, **EIa**, and **ES**. Atom colors: S (yellow), O (red), N (blue), C (black), H (white). Protein backbone is shown as transparent ribbons.[133] Reprinted with permission from J. Phys. Chem. B 2018;122:4299 Copyright (2018) American Chemical Society.

TASS was also used in the study of Mg^{2+} assisted pyrophosphate release in a sugar nucleotidyltransferase. [134] In that work, 10 CVs were chosen, which included several torsional angles of the side-chain residues which interacted with the pyrophosphate. It was shown that US predicts a slightly different mechanism and a higher free energy barrier

compared to TASS as a result of poor sampling of orthogonal coordinates by the former method. Sahoo and Nair used TASS to simulate proton exchange reaction between methane and acid-sites within the H-ZSM-5 zeolite using DFT based QM/polarized-MM simulations. [135] Without invoking a controlled sampling of distance between CH_4 and the acid site in zeolite, CH_4 molecule diffuses away from the acid-sites during the simulation. By the virtue of the umbrella-bias in the TASS formulation, controlled sampling of this coordinate could be carried out, thus making the free-energy computations highly efficient.

6 | CONCLUSIONS

Accelerating large number of CVs and thus exploring a high-dimensional free-energy landscape is crucial to to obtain a quick free-energy convergence in MD simulations. Conventional methods like US and metadynamics are inefficient in exploring high-dimensional landscapes, as sampling efficiency decreases exponentially with the number of CVs. We have discussed four promising methods in detail which mitigate the limitations imposed by the dimensionality of the CV-space.

BEMetaD is quite popular today and is mostly applied to study wide variety of problems in bimolecular systems. However, the main limitation of this method is the need of replica-exchange which requires overlapping probability distributions between two replicas. This decreases the computational efficiency of the method. As a result, BEMetaD based AIMD simulation of chemical reaction in soft matter systems has not been reported yet. PBMetaD alleviates this problem by parallel sampling of CVs within single replica. PBMetaD has the scope of sampling large number of CVs, and has been also used in studying conformational changes in bimolecular systems and chemical reactions using AIMD (with semi-empirical Hamiltonian). Efficiency of PBMetaD would also diminish with the increase of number of CVs due to the mutually dependent scaling of biases. On the other hand, TAMD/d-AFED approach is shown to be very powerful in enhanced sampling with a few hundreds of CVs. However, TAMD/d-AFED method should be carefully carried out as maintaining adiabatic separation between CV subsystem and physical subsystem is vital. Further, increasing CV temperature can result in unphysical structural changes, especially when the force-fields are not designed to operate at high temperatures. TAMD/d-AFED method has been used in AIMD simulations, conformational sampling in biomolecular systems and crystal structure predictions. On the other hand, all the three methods discussed above can become inefficient in exploring free-energy basins that are broad and unbound. A controlled sampling of CVs is preferred to avoid sampling myriad of uninteresting configurations. This is achieved in the relatively new TASS sampling method which combines US, metadynamics and TAMD/d-AFED. The method has been shown to be powerful for computing high-dimensional free-energy surfaces of chemical reactions, including enzymatic reactions. Even the computationally expensive DFT based QM/MM methods have been used with TASS and a quick free-energy convergence was reported. One of the shortcoming of TASS is that prior chemical knowledge is required to select the type of biasing along the CVs in an efficient manner.

A variety of problems like protein-folding, ligand binding in proteins and nucleic acids, structural refinements of biomolecules based on experimental data, crystal structure predictions, exploration of reaction pathways, and modeling of enzymatic reactions require quick sampling of large number of transverse CVs, which can now be studied using the aforementioned methods. Combining these CV-based approaches with global-tempering methods could further strengthen these computational methods to study more complex problems.

ACKNOWLEDGEMENTS

Authors thank Department of Biotechnology for funding. SA thanks IIT Kanpur for her Ph.D. fellowship.

REFERENCES

[1] Peters B. Reaction Rate Theory and Rare Events. Amsterdam, Netherlands: Elsevier; 2017.

[2] Tuckerman ME. Statistical Mechanics: Theory and Molecular Simulation. 1st ed. Oxford: Oxford University Press; 2010.

[3] Vanden-Eijnden E. Some Recent Techniques for Free Energy Calculations. J Comput Chem 2009;30:1737.

[4] Christ CD, Mark AE, van Gunsteren WF. Basic ingredients of free energy calculations: A review. J Comput Chem 2010;31:1569–1582.

[5] Bonella S, Meloni S, Ciccotti G. Theory and Methods for Rare Events. Eur Phys J B 2012;85:97.

[6] Valsson O, Tiwary P, Parrinello M. Enhancing Important Fluctuations: Rare Events and Metadynamics from a Conceptual Viewpoint. Annu Rev Phys Chem 2016;67:159.

[7] Torrie GM, Valleau JP. Monte Carlo Free Energy Estimates Using Non-Boltzmann Sampling: Application to the Subcritical Lennard-Jones Fluid. Chem Phys Lett 1974;28:578.

[8] Laio A, VandeVondele J, Rothlisberger U. A Hamiltonian Electrostatic Coupling Scheme for Hybrid Car-Parrinello Molecular Dynamics Simulations. J Chem Phys 2002;116:6941.

[9] Iannuzzi M, Laio A, Parrinello M. Efficient Exploration of Reactive Potential Energy Surfaces Using Car-Parrinello Molecular Dynamics. Phys Rev Lett 2003;90:238302.

[10] Valsson O, Parrinello M. Variational Approach to Enhanced Sampling and Free Energy Calculations. Phys Rev Lett 2014;113:090601.

[11] Carter E, Ciccotti G, Hynes J, Karpal R. Constrained reaction coordinate dynamics for the simulation of rare events. Chem Phys Lett 1989;156:472.

[12] Comer J, Gumbart JC, Hénin J, Lelièvre T, Pohorille A, Chipot C. The Adaptive Biasing Force Method: Everything You Always Wanted To Know but Were Afraid To Ask. J Phys Chem B 2015;119:1129.

[13] Rosso L, Mináry P, Zhu Z, Tuckerman ME. On the use of the adiabatic molecular dynamics technique in the calculation of free energy profiles. J Chem Phys 2002;116:4389.

[14] Affentranger R, Tavernelli I, Di Iorio EE. A Novel Hamiltonian Replica Exchange MD Protocol to Enhance Protein Conformational Space Sampling. J Chem Theory Comput 2006;2:217.

[15] Liu P, Kim B, Friesner RA, Berne BJ. Replica exchange with solute tempering: A method for sampling biological systems in explicit water. Proc Nat Acad Sci 2005;102:13749–13754.

[16] Gao YQ. An integrate-over-temperature approach for enhanced sampling. J Chem Phys 2008;128:064105.

[17] Grubmüller H. Predicting slow structural transitions in macromolecular systems: Conformational flooding. Phys Rev E 1995;52:2893.

[18] Hamelberg D, Mongan J, McCammon JA. Accelerated Molecular Dynamics: A Promising and Efficient Simulation Method for Biomolecules. J Chem Phys 2004;120:11919–11929.

[19] Sugita Y, Okamoto Y. Replica-exchange molecular dynamics method for protein folding. Chem Phys Lett 1999;314:141.

[20] Lelièvre T, Rousset M, Stoltz G. Free Energy Computations: A Mathematical Perspective. London: Imperial College Press; 2010.

[21] Pietrucci F. Strategies for the exploration of free energy landscapes: Unity in diversity and challenges ahead. Rev Phys 2017;2:32–45.

[22] Abrams C, Bussi G. Enhanced Sampling in Molecular Dynamics Using Metadynamics, Replica-Exchange, and Temperature-Acceleration. Entropy 2014;16:163.

[23] Christ CD, Mark AE, van Gunsteren WF. Basic Ingredients of Free Energy Calculations: A Review. J Comput Chem 2010;31:1569.

[24] Laio A, Parrinello M. Escaping Free-energy Minima. Proc Natl Acad Sci USA 2002;99:12562.

[25] Laio A, Parrinello M. Computing free energies and accelerating rare events with metadynamics, vol. 1. Ferrario M, Ciccotti G, Binder K, editors, Berlin: Springer; 2006.

[26] Ensing B, Vivo MD, Liu Z, Moore P, Klein ML. Metadynamics as a Tool for Exploring Free Energy Landscapes of Chemical Reactions. Acc Chem Res 2006;39:73.

[27] Barducci A, Bonomi M, Parrinello M. Metadynamics. WIREs Comput Mol Sci 2011;1:826.

[28] Laio A, Gervasio FL. Metadynamics: a method to simulate rare events and reconstruct the free energy in biophysics, chemistry and material science. Rep Prog Phys 2008;71:126601.

[29] Sutto L, Marsili S, Gervasio FL. New advances in metadynamics. Wiley Interdiscip Rev Comput Mol Sci 2012;2:771–779.

[30] Bussi G, Branduardi D. 1. In: Free-Energy Calculations with Metadynamics: Theory and Practice Wiley-Blackwell; 2015. p. 1–49.

[31] Barducci A, Bussi G, Parrinello M. Well-Tempered Metadynamics: A Smoothly Converging and Tunable Free-Energy Method. Phys Rev Lett 2008;100:020603.

[32] Branduardi D, Bussi G, Parrinello M. Metadynamics with Adaptive Gaussians. J Chem Theory Comput 2012;8:2247.

[33] Dama JF, Parrinello M, Voth GA. Well-Tempered Metadynamics Converges Asymptotically. Phys Rev Lett 2014;112:240602.

[34] Bian Y, Zhang J, Wang J, Wang W. On the accuracy of metadynamics and its variations in a protein folding process. Mol Simul 2015;41:752–763.

[35] Piana S, Laio A. A Bias-Exchange Approach to Protein Folding. J Phys Chem B 2007;111:4553.

[36] Galvelis R, Sugita Y. Replica State Exchange Metadynamics for Improving the Convergence of Free Energy Estimates. J Comput Chem 2015;36:1446–1455.

[37] Baftizadeh F, Cossio P, Pietrucci F, Laio A. Protein Folding and Ligand-Enzyme Binding from Bias-Exchange Metadynamics Simulations. Curr Phys Chem 2012;2:79–91.

[38] Kumar S, Rosenberg JM, Bouzida D, Swendsen RH, Kollman PA. The Weighted Histogram Analysis Method for Free-energy Calculations on Biomolecules. I. The Method. J Comput Chem 1992;13:1011.

[39] Biarnes X, Pietrucci F, Marinelli F, Laio A. METAGUI. A VMD interface for analyzing metadynamics and molecular dynamics simulations. Comput Phys Commun 2012;183:203–211.

[40] Yu H, Lin YS. Toward structure prediction of cyclic peptides. Phys Chem Chem Phys 2015;17:4210–4219.

[41] Awasthi S, Kapil V, Nair NN. Sampling Free Energy Surfaces as Slices by Combining Umbrella Sampling and Metadynamics. J Comput Chem 2016;37:1413.

[42] Marinelli F, Pietrucci F, Laio A, Piana S. A Kinetic Model of Trp-Cage Folding from Multiple Biased Molecular Dynamics Simulations. PLoS Comput Biol 2009;5:e1000452.

[43] Delor M, Dai J, Roberts TD, Rogers JR, Hamed SM, Neaton JB, et al. Exploiting Chromophore-Protein Interactions through Linker Engineering To Tune Photoinduced Dynamics in a Biomimetic Light-Harvesting Platform. J Am Chem Soc 2018;140:6278–6287.

[44] Mlýnský V, Bussi G. Molecular Dynamics Simulations Reveal an Interplay between SHAPE Reagent Binding and RNA Flexibility. J Phys Chem Lett 2018;9:313–318.

[45] Bian Y, Tan C, Wang J, Sheng Y, Zhang J, Wang W. Atomistic Picture for the Folding Pathway of a Hybrid-1 Type Human Telomeric DNA G-quadruplex. PLoS Comput Biol 2014;10.

[46] Bian Y, Zhang J, Wang J, Wang J, Wang W. Free Energy Landscape and Multiple Folding Pathways of an H-Type RNA Pseudoknot. PLoS One 2015;10.

[47] Pietrucci F, Marinelli F, Carloni P, Laio A. Substrate Binding Mechanism of HIV-1 Protease from Explicit-Solvent Atomistic Simulations. J Am Chem Soc 2009;131:11811–11818.

[48] Herbert C, Schieborr U, Saxena K, Juraszek J, Smet F, Alcouffe C, et al. Molecular Mechanism of SSR128129E, an Extracellularly Acting, Small-Molecule, Allosteric Inhibitor of FGF Receptor Signaling. Cancer Cell 2013;23:489 – 501.

[49] Li Y, Lavey NP, Coker JA, Knobbe JE, Truong DC, Yu H, et al. Consequences of Depsipeptide Substitution on the ClpP Activation Activity of Antibacterial Acyldepsipeptides. ACS Med Chem Lett 2017;8:1171–1176.

[50] Duan M, Liu N, Zhou W, Li D, Yang M, Hou T. Structural Diversity of Ligand-Binding Androgen Receptors Revealed by Microsecond Long Molecular Dynamics Simulations and Enhanced Sampling. J Chem Theory and Comput 2016;12:4611–4619.

[51] Paloncýová M, Navrátilová V, Berka K, Laio A, Otyepka M. Role of Enzyme Flexibility in Ligand Access and Egress to Active Site: Bias-Exchange Metadynamics Study of 1,3,7-Trimethyluric Acid in Cytochrome P450 3A4. J Chem Theory and Comput 2016;12:2101–2109.

[52] Zhu L, Jiang H, Sheong FK, Cui X, Gao X, Wang Y, et al. A Flexible Domain-Domain Hinge Promotes an Induced-fit Dominant Mechanism for the Loading of Guide-DNA into Argonaute Protein in Thermus thermophilus. J Phys Chem B 2016;120:2709–2720.

[53] Marinelli F, Kuhlmann SI, Grell E, Kunte HJ, Ziegler C, Faraldo-Gómez JD. Evidence for an allosteric mechanism of substrate release from membrane-transporter accessory binding proteins. Proc Natl Acad Sci 2011;108:E1285–E1292.

[54] Bisha I, Rodriguez A, Laio A, Magistrato A. Metadynamics Simulations Reveal a Na+ Independent Exiting Path of Galactose for the Inward-Facing Conformation of vSGLT. PLoS Comput Biol 2014 12;10:1–8.

[55] Thyparambil AA, Bazin I, Guiseppi-Elie A. Evaluation of Ochratoxin Recognition by Peptides Using Explicit Solvent Molecular Dynamics. Toxins 2017;9.

[56] Galassi VV, Arantes GM. Partition, orientation and mobility of ubiquinones in a lipid bilayer. Biochim Biophys Acta, Bioenerg 2015;1847:1560 – 1573.

[57] Żołnowska B, Sławiński J, Szafrański K, Angeli A, Supuran CT, Kawiak A, et al. Novel 2-(2-arylmethylthio-4-chloro-5-methylbenzenesulfonyl)-1-(1,3,5-triazin-2-ylamino)guanidine derivatives: Inhibition of human carbonic anhydrase cytosolic isozymes I and II and the transmembrane tumor-associated isozymes IX and XII, anticancer activity, and molecular modeling studies. Eur J Med Chem 2018;143:1931 – 1941.

[58] Cunha RA, Bussi G. Unraveling Mg2+-RNA binding with atomistic molecular dynamics. RNA 2017;23:628–638.

[59] Piana S, Laio A. Advillin Folding Takes Place on a Hypersurface of Small Dimensionality. Phys Rev Lett 2008;101:208101.

[60] Piana S, Laio A, Marinelli F, Troys MV, Bourry D, Ampe C, et al. Predicting the Effect of a Point Mutation on a Protein Fold: The Villin and Advillin Headpieces and Their Pro62Ala Mutants. J Mol Biol 2008;375:460 – 470.

[61] Todorova N, Marinelli F, Piana S, Yarovsky I. Exploring the Folding Free Energy Landscape of Insulin Using Bias Exchange Metadynamics. J Phys Chem B 2009;113:3556–3564.

[62] Pietrucci F, Laio A. A Collective Variable for the Efficient Exploration of Protein Beta-Sheet Structures: Application to SH3 and GB1. J Chem Theory Comput 2009;5:2197–2201.

[63] Juraszek J, Bolhuis PG. (Un)Folding Mechanisms of the FBP28 WW Domain in Explicit Solvent Revealed by Multiple Rare Event Simulation Methods. Biophys J 2010;98:646–656.

[64] Cossio P, Marinelli F, Laio A, Pietrucci F. Optimizing the Performance of Bias-Exchange Metadynamics: Folding a 48-Residue LysM Domain Using a Coarse-Grained Model. J Phys Chem B 2010;114:3259–3265.

[65] Rossetti G, Cossio P, Laio A, Carloni P. Conformations of the Huntingtin N-term in aqueous solution from atomistic simulations. FEBS Letters 2011;585:3086–3089.

[66] Granata D, Camilloni C, Vendruscolo M, Laio A. Characterization of the free-energy landscapes of proteins by NMR-guided metadynamics. Proc Natl Acad Sci 2013;110:6817–6822.

[67] Benetti F, Biarnes X, Attanasio F, Giachin G, Rizzarelli E, Legname G. Structural Determinants in Prion Protein Folding and Stability. J Mol Bol 2014;426:3796–3810.

[68] Rogers JR, McHugh SM, Lin YS. Predictions for α-Helical Glycopeptide Design from Structural Bioinformatics Analysis. J Chem Inf Model 2017;57:2598–2611.

[69] Ansari SM, Coletta A, Kirkeby Skeby K, Sørensen J, Schiøtt B, Palmer DS. Allosteric-Activation Mechanism of Bovine Chymosin Revealed by Bias-Exchange Metadynamics and Molecular Dynamics Simulations. J Phys Chem B 2016;120:10453–10462.

[70] McHugh SM, Rogers JR, Yu H, Lin YS. Insights into How Cyclic Peptides Switch Conformations. J Chem Theory and Comput 2016;12:2480–2488.

[71] Slough DP, Yu H, McHugh SM, Lin YS. Toward accurately modeling N-methylated cyclic peptides. Phys Chem Chem Phys 2017;19:5377–5388.

[72] Michel J, Cuchillo R. The Impact of Small Molecule Binding on the Energy Landscape of the Intrinsically Disordered Protein C-Myc. PLsS One 2012 07;7:1–13.

[73] Damas JM, Filipe LCS, Campos SRR, Lousa D, Victor BL, Baptista AM, et al. Predicting the Thermodynamics and Kinetics of Helix Formation in a Cyclic Peptide Model. J Chem Theory Comput 2013;9:5148–5157.

[74] Mahajan SP, Velez-Vega C, Escobedo FA. Tilting the Balance between Canonical and Noncanonical Conformations for the H1 Hypervariable Loop of a Llama VHH through Point Mutations. J Phys Chem B 2013;117:13–24.

[75] Do TN, Choy WY, Karttunen M. Accelerating the Conformational Sampling of Intrinsically Disordered Proteins. J Chem Theory Comput 2014;10:5081–5094.

[76] Zerze GH, Miller CM, Granata D, Mittal J. Free Energy Surface of an Intrinsically Disordered Protein: Comparison between Temperature Replica Exchange Molecular Dynamics and Bias-Exchange Metadynamics. J Chem Theory Comput 2015;11:2776–2782.

[77] Camilloni C, Vendruscolo M. Statistical Mechanics of the Denatured State of a Protein Using Replica-Averaged Metadynamics. J Am Chem Soc 2014;136:8982–8991.

[78] Camilloni C, Vendruscolo M. Using Pseudocontact Shifts and Residual Dipolar Couplings as Exact NMR Restraints for the Determination of Protein Structural Ensembles. Biochemistry 2015;54:7470–7476.

[79] cheng Chiu C, Singh S, de Pablo J. Effect of Proline Mutations on the Monomer Conformations of Amylin. Biophys J 2013;105:1227 – 1235.

[80] Pietrucci F, Mollica L, Blackledge M. Mapping the Native Conformational Ensemble of Proteins from a Combination of Simulations and Experiments: New Insight into the src-SH3 Domain. J Phys Chem Lett 2013;4:1943–1948.

[81] Corbi-Verge C, Marinelli F, Zafra-Ruano A, Ruiz-Sanz J, Luque I, Faraldo-Gómez JD. Two-state dynamics of the SH3–SH2 tandem of Abl kinase and the allosteric role of the N-cap. Proc Natl Acad Sci 2013;110:E3372–E3380.

[82] Buchanan LE, Dunkelberger EB, Tran HQ, Cheng PN, Chiu CC, Cao P, et al. Mechanism of IAPP amyloid fibril formation involves an intermediate with a transient-sheet. Proc Natl Acad Sci 2013;110:19285–19290.

[83] Scarabelli G, Provasi D, Negri A, Filizola M. Bioactive Conformations of Two Seminal Delta Opioid Receptor Penta-Peptides Inferred from Free-Energy Profiles. Biopolymers 2014;101:21–27.

[84] Ceballos JA, Giraldo MA, Cossio P. Effects of a disulfide bridge prior to amyloid formation of the ABRI peptide. RSC Adv 2014;4:36923–36928.

[85] Li D, Liu M, Ji B. Mapping the Dynamics Landscape of Conformational Transitions in Enzyme: The Adenylate Kinase Case. Biophys J 2015;109:647 – 660.

[86] Hoffmann KQ, McGovern M, Chiu Cc, de Pablo JJ. Secondary Structure of Rat and Human Amylin across Force Fields. PLoS One 2015;10.

[87] Gomez-Sicilia A, Sikora M, Cieplak M, Carrion-Vazquez M. An Exploration of the Universe of Polyglutamine Structures. PLoS Comput Biol 2015;11.

[88] Cristina P, Michela G, Laura B, Andrea S, Giovanna M. Metadynamics Simulations Rationalise the Conformational Effects Induced by N-Methylation of RGD Cyclic Hexapeptides. Chem Eur J 2015;21:14165–14170.

[89] Camilloni C, Sala BM, Sormanni P, Porcari R, Corazza A, De Rosa M, et al. Rational design of mutations that change the aggregation rate of a protein while maintaining its native structure and stability. Sci Rep 2016;6.

[90] Singh R, Bansal R, Rathore AS, Goel G. Equilibrium Ensembles for Insulin Folding from Bias-Exchange Metadynamics. Biophys J 2017;112:1571–1585.

[91] Domene C, Barbini P, Furini S. Bias-Exchange Metadynamics Simulations: An Efficient Strategy for the Analysis of Conduction and Selectivity in Ion Channels. J Chem Theory Comput 2015;11:1896–1906.

[92] Furini S, Domene C. Computational studies of transport in ion channels using metadynamics. Biochim Biophys Acta, Biomembr 2016;1858:1733 – 1740.

[93] Jorgensen C, Furini S, Domene C. Energetics of Ion Permeation in an Open-Activated TRPV1 Channel. Biophys J 2016;111:1214–1222.

[94] Borkar AN, Vallurupalli P, Camilloni C, Kay LE, Vendruscolo M. Simultaneous NMR characterisation of multiple minima in the free energy landscape of an RNA UUCG tetraloop. Phys Chem Chem Phys 2017;19:2797–2804.

[95] Liu N, Duan M, Yang M. Structural Properties of Human IAPP Dimer in Membrane Environment Studied by All-Atom Molecular Dynamics Simulations. Sci Rep 2017;7.

[96] McGovern M, Abbott N, Pablo J. Dimerization of Helical β-Peptides in Solution. Biophys J 2012;102:1435 – 1442.

[97] Baftizadeh F, Pietrucci F, Biarnés X, Laio A. Nucleation Process of a Fibril Precursor in the C-Terminal Segment of Amyloid-β. Phys Rev Lett 2013;110:168103.

[98] Chiu Cc, de Pablo JJ. Fibrillar dimer formation of islet amyloid polypeptides. AIP Adv 2015;5.

[99] Borkar AN, Bardaro MF, Camilloni C, Aprile FA, Varani G, Vendruscolo M. Structure of a low-population binding intermediate in protein-RNA recognition. Proc Natl Acad Sci 2016;113:7171–7176.

[100] Lousa D, Pinto ART, Victor BL, Laio A, Veiga AS, Castanho MARB, et al. Fusing simulation and experiment: The effect of mutations on the structure and activity of the influenza fusion peptide. Sci Rep 2016;6.

[101] Pfaendtner J, Bonomi M. Efficient Sampling of High-Dimensional Free-Energy Landscapes with Parallel Bias Metadynamics. J Chem Theory Comput 2015;11:5062.

[102] Heller GT, Aprile FA, Bonomi M, Camilloni C, Simone AD, Vendruscolo M. Sequence Specificity in the Entropy-Driven Binding of a Small Molecule and a Disordered Peptide. J Mol Biol 2017;429:2772–2779.

[103] Löhr T, Jussupow A, Camilloni C. Metadynamic metainference: Convergence towards force field independent structural ensembles of a disordered peptide. J Chem Phys 2017;146:165102.

[104] Prakash A, Baer MD, Mundy CJ, Pfaendtner J. Peptoid Backbone Flexibilility Dictates Its Interaction with Water and Surfaces: A Molecular Dynamics Investigation. Biomacromolecules 2018;19(3):1006–1015. https://doi.org/10.1021/acs.biomac.7b01813, pMID: 29443506.

[105] Fu CD, Pfaendtner J. Lifting the Curse of Dimensionality on Enhanced Sampling of Reaction Networks with Parallel Bias Metadynamics. J Chem Theory Comput 2018;14:2516–2525.

[106] Pietrucci F, Andreoni W. Graph Theory Meets Ab Initio Molecular Dynamics: Atomic Structures and Transformations at the Nanoscale. Phys Rev Lett 2011;107:85504.

[107] Rosso L, Abrams JB, Tuckerman ME. Mapping the Backbone Dihedral Free-Energy Surfaces in Small Peptides in Solution Using Adiabatic Free-Energy Dynamics. J Phys Chem B 2005;109:4162.

[108] Maragliano L, Vanden-Eijnden E. A Temperature Accelerated Method for Sampling Free Energy and Determining Reaction Pathways in Rare Events Simulations. Chem Phys Lett 2006;426:168.

[109] Abrams JB, Tuckerman ME. Efficient and Direct Generation of Multidimensional Free Energy Surfaces via Adiabatic Dynamics without Coordinate Transformations. J Phys Chem B 2008;112:15742.

[110] Cuendet MA, Tuckerman ME. Free Energy Reconstruction from Metadynamics or Adiabatic Free Energy Dynamics Simulations. J Chem Theory Comput 2014;10:2975.

[111] Yu TQ, Tuckerman ME. Temperature-Accelerated Method for Exploring Polymorphism in Molecular Crystals Based on Free Energy. Phys Rev Lett 2011;107:015701.

[112] Abrams CF, Vanden-Eijnden E. Large-scale conformational sampling of proteins using temperature-accelerated molecular dynamics. Proc Natl Acad Sci 2010;107:4961–4966.

[113] Vashisth H, Maragliano L, Abrams CF. DFG-Flip in the Insulin Receptor Kinase Is Facilitated by a Helical Intermediate State of the Activation Loop. Biophys J 2012;102:1979 – 1987.

[114] Maragliano L, Cottone G, Ciccotti G, Vanden-Eijnden E. Mapping the Network of Pathways of CO Diffusion in Myoglobin. J Am Chem Soc 2010;132:1010–1017.

[115] Lapelosa M, Abrams CF. A Computational Study of Water and CO Migration Sites and Channels Inside Myoglobin. J Chem Theory Comput 2013;9:1265–1271.

[116] Tzanov AT, Cuendet MA, Tuckerman ME. How Accurately Do Current Force Fields Predict Experimental Peptide Conformations? An Adiabatic Free Energy Dynamics Study. J Phys Chem B 2014;118:6539–6552.

[117] Cortes-Ciriano I, Bouvier G, Nilges M, Maragliano L, Malliavin TE. Temperature Accelerated Molecular Dynamics with Soft-Ratcheting Criterion Orients Enhanced Sampling by Low-Resolution Information. J Chem Theory Comput 2015;11:3446–3454.

[118] Geslin PA, Ciccotti G, Meloni S. An observable for vacancy characterization and diffusion in crystals. J Chem Phys 2013;138:144103.

[119] Lucid J, Meloni S, MacKernan D, Spohr E, Ciccotti G. Probing the Structures of Hydrated Nafion in Different Morphologies Using Temperature-Accelerated Molecular Dynamics Simulations. J Phys Chem C 2013;117:774–782.

[120] Yu TQ, Chen PY, Chen M, Samanta A, Vanden-Eijnden E, Tuckerman M. Order-parameter-aided temperature-accelerated sampling for the exploration of crystal polymorphism and solid-liquid phase transitions. J Chem Phys 2014;140:214109.

[121] E Schneider MET L Vogt. Exploring polymorphism of benzene and naphthalene with free energy based enhanced molecular dynamics. Acta Crystallogr B 2016;72:542–550.

[122] Samanta A, Morales MA, Schwegler E. Exploring the free energy surface using ab initio molecular dynamics. J Chem Phys 2016;144:164101.

[123] Shtukenberg AG, Zhu Q, Carter DJ, Vogt L, Hoja J, Schneider E, et al. Powder diffraction and crystal structure prediction identify four new coumarin polymorphs. Chem Sci 2017;8:4926–4940.

[124] Chen M, Cuendet MA, Tuckerman ME. Heating and Flooding: A Unified Approach for Rapid Generation of Free Energy Surfaces. J Chem Phys 2012;137:024102.

[125] Samanta A, Chen M, Yu TQ, Tuckerman M, E W. Sampling saddle points on a free energy surface. J Chem Phys 2014;140:164109.

[126] Chen M, Yu TQ, Tuckerman ME. Locating Landmarks on High-Dimensional Free Energy Surfaces. Proc Natl Acad Sci 2015;112:3235.

[127] Abrams JB, Rosso L, Tuckerman ME. Efficient and precise solvation free energies via alchemical adiabatic molecular dynamics. J Chem Phys 2006;125:074115.

[128] Cuendet MA, Tuckerman ME. Alchemical Free Energy Differences in Flexible Molecules from Thermodynamic Integration or Free Energy Perturbation Combined with Driven Adiabatic Dynamics. J Chem Theory Comput 2012;8:3504–3512.

[129] Cuendet MA, Margul DT, Schneider E, Vogt-Maranto L, Tuckerman ME. Endpoint-restricted adiabatic free energy dynamics approach for the exploration of biomolecular conformational equilibria. J Chem Phys 2018;149:072316.

[130] Ferrenberg AM, Swendsen RH. Optimized Monte Carlo Data Analysis. Phys Rev Lett 1989;63:1195.

[131] Kästner J. Umbrella Sampling. WIREs Comput Mol Sci 2011;1:932.

[132] Awasthi S, Nair NN. Exploring High Dimensional Free Energy Landscapes: Temperature Accelerated Sliced Sampling. J Chem Phys 2017;146:094108.

[133] Awasthi S, Gupta S, Tripathi R, Nair NN. Mechanism and Kinetics of Aztreonam Hydrolysis Catalyzed by Class-C β-Lactamase: A Temperature-Accelerated Sliced Sampling Study. J Phys Chem B 2018;122:4299–4308.

[134] Vithani N, Jagtap PKA, Verma SK, Tripathi R, Awasthi S, Nair NN, et al. Mechanism of Mg2+-Accompanied Product Release in Sugar Nucleotidyltransferases. Structure 2018;26:459 – 466.

[135] Sahoo SK, Nair NN. Interfacing the Core-Shell or the Drude Polarizable Force Field With Car-Parrinello Molecular Dynamics for QM/MM Simulations. Front Chem 2018;6:275.